

Article

Engineered Stone Produced with Glass Packaging Waste, Quartz Powder, and Epoxy Resin

Gabriela Nunes Sales Barreto ^{1,*}, Elaine Aparecida Santos Carvalho ¹, Vitor da Silva de Souza ¹, Maria Luiza Pessanha Menezes Gomes ¹, Afonso R. G. de Azevedo ², Sérgio Neves Monteiro ³ and Carlos Maurício Fontes Vieira ¹

- ¹ Advanced Materials Laboratory (LAMAV), State University of Northern Fluminense–UENF, Av. Alberto Lamego, 2000, Campos dos Goytacazes 28013-602, RJ, Brazil; elainesanttos@yahoo.com.br (E.A.S.C.); vitor.silvasouza_@hotmail.com (V.d.S.d.S.); malu_pmg@hotmail.com (M.L.P.M.G.); vieira@uenf.br (C.M.F.V.)
- ² Civil Engineering Laboratory (LECIV), State University of the Northern Rio de Janeiro-UENF, Av. Alberto Lamego, 2000, Campos dos Goytacazes 28013-602, RJ, Brazil; afonso@uenf.br
- ³ Department of Materials Science, Instituto Militar de Engenharia–IME, Praça General Tibúrcio, 80, Praia Vermelha, Urca, Rio de Janeiro 22290-270, RJ, Brazil; snevesmonteiro@gmail.com
- * Correspondence: gabibarroto.93@gmail.com

Abstract: Engineered stone (ENS) is a type of artificial stone composed of stone wastes bonded together by a polymeric matrix. ENS presents a profitable alternative for solid waste management, since its production adds value to the waste by reusing it as raw material and reduces environmental waste disposal. The present work's main goal is to produce an ENS based on quartz powder waste, glass packaging waste, and epoxy resin. The wastes were size-distributed by the fine sieving method. Then, the closest-packed granulometric mixture, as well as the minimum amount of resin that would fill the voids of these mixtures, was calculated. ENS plates were prepared with 15%wt (ENS-15) and 20%wt (ENS-20) epoxy resin by vibration, compression (10 tons for 20 min at 90 °C), and vacuum of 600 mmHg. The plates were sanded and cut for physical, chemical, and mechanical tests. Scanning electron microscopy analysis of fractured specimens was performed. ENS-15 presented 2.26 g/cm³ density, 0.1% water absorption, 0.21% apparent porosity, and 33.5 MPa bend strength and was resistant to several chemical and staining agents. The results classified ENS as a high-quality coating material, technically and economically viable, with properties similar to commercial artificial stones. Therefore, the development of ENS based on waste glass and quartz powder meets the concept of sustainable development, as this proposed novel material could be marketed as a building material and simultaneously minimize the amount of these wastes that are currently disposed of in landfills.

Keywords: engineered stone; wastes; waste glass; quartz; epoxy resin



Citation: Barreto, G.N.S.; Carvalho, E.A.S.; Souza, V.d.S.d.; Gomes, M.L.P.M.; de Azevedo, A.R.G.; Monteiro, S.N.; Vieira, C.M.F. Engineered Stone Produced with Glass Packaging Waste, Quartz Powder, and Epoxy Resin. *Sustainability* **2022**, *14*, 7227. <https://doi.org/10.3390/su14127227>

Academic Editor: Mariateresa Lettieri

Received: 31 March 2022

Accepted: 8 June 2022

Published: 13 June 2022

Publisher's Note: MDPI stays neutral with regard to jurisdictional claims in published maps and institutional affiliations.



Copyright: © 2022 by the authors. Licensee MDPI, Basel, Switzerland. This article is an open access article distributed under the terms and conditions of the Creative Commons Attribution (CC BY) license (<https://creativecommons.org/licenses/by/4.0/>).

1. Introduction

An enormous issue with glass is its one-time use, such as in beverage packaging, squandering a non-biodegradable material that occupies significant space in landfills, reinforcing the reliance on natural resources, and causing damage to the environment [1]. Moreover, dumping glass waste in landfills adds to the disposal issue that is disturbing the biological equilibrium all over the planet [2].

Waste glass, in theory, after sorting and cleaning, could be remelted to manufacture new glass products. However, its variety of colors and contaminations makes recycling laborious, reducing the glass recycling rate. Thereby, waste glass is frequently sent to landfills, contaminating nature, harming the environment, and wasting resources. Around the globe, it is estimated that a whopping amount of glass waste is landfilled each year, approximately 200 million tons, drawing international attention and efforts to develop novel products based on waste glass [3].

Compared to other wastes, such as wood and plastic, waste glass presents chemical stability, which makes its reuse in the manufacture of construction materials of great interest due to some advantages over recycling, such as low energy consumption (as it does not need melting) and simplicity in the treatment of waste [4].

Another material that takes a million years to decompose, generating environmental harm when wrongly disposed of, is quartz powder, composed of 99.0% SiO₂, 0.8% Al₂O₃, 0.1% Fe₂O₃, and 0.1% TiO₂ [5].

Wastes, in general, are nowadays a huge challenge for the industrialized world, since they are usually discarded as useless due to poor technological handling [6]. Improperly disposed of wastes generate a series of disorders, such as destruction of landscape, fauna and flora, air and soil contamination, and populational health risks [7]. For that reason, it is important to propose new sustainable approaches for waste management, representing consistent and effective ways of minimizing these impacts [8].

In that scenario, reusing waste materials in building materials has been attracting research interests, aiming to diminish natural resources wastage, manufacturing costs, and landfilling [9]. With regard to civil construction, waste recycling at any stage would provide sustainable development in this sector, which is considered to be a major waste generator among the macro sectors of the economy, since its consumption of natural resources is approximately 75% [10].

In this sense, the combination of the construction industry with the reuse of waste has become one of the main directions of research [5], with the replacement of raw materials from civil construction with waste products encouraged by the industry, aiming to promote sustainability [11].

Among the civil construction materials, a possible solution to reuse glass and quartz wastes is the development of a novel composite material, called engineered stone (ENS), artificial stones manufactured with a high amount of fine mineral agglomerated polymeric resins [6].

In this way, particulate natural materials of ENS can be substituted by wastes. The wastes are crushed in different granulometries and mixed with resins and additives. This mixture forms a mass that goes through a molding process by means of vibration, compression, and vacuum. The thermosetting resin contained in the paste undergoes a hardening process resulting in the ENS, with dimensions defined by the mold size [12].

Lee and Shin [13] reported on the influence of vacuum, mold temperature, and cooling rate on the production of fiberglass/PET composites. It was observed that specimens preheated without vacuum registered 1.9% porosity, while those made with vacuum registered only 0.3–0.4% porosity. Vacuum-processed samples also achieved better tensile strength values, increasing from 141 Mpa (without vacuum) to 258 Mpa (with vacuum). The authors concluded that the vacuum decreases the porosity, consequently improving the composite's mechanical properties.

Lee et al. [14] studied the effects of compaction pressure, vacuum level, and vibration frequency on the properties of artificial stones produced by vacuum vibrocompression. The authors observed that by increasing the compaction pressure (up to a certain limit), vacuum and vibration diminish porosity and water absorption, enhancing the mechanical properties.

Several studies have proposed the reuse of natural wastes such as marbles, granites, quartzites, and brick waste [14–19] agglomerated by polymeric matrixes, such as epoxy and polyester, to develop engineered stones, producing stones with better mechanical, physical, and chemical properties compared to artificial and natural stones on the market.

This research is focused on producing ENS with quartz powder combined with colorless glass waste from beverage packaging. The decision to use only colorless glass came from the concern with the aesthetic appeal of the final product, since artificial stones with the highest market value are white. The use of glass from beverage packaging had the purpose of finding a sustainable destination for this single-use glass product.

This research's main goal is to confirm the technical feasibility of a novel ENS produced with beverage packaging waste, quartz powder waste, and epoxy resin. The investment in the ENS development could reinsert waste into a manufacturing process along with moving the economy by entering an unexplored and growing industrial area in Brazil [19].

2. Materials and Methods

2.1. Materials

The colorless beverage glass packaging was collected by the authors in bars and supermarkets located in Campos dos Goytacazes, RJ, Brazil. The quartz dust was supplied by EcologicStone, an artificial stone company located in Cachoeiro de Itapemirim, ES, Brazil. The epoxy resin (MC130) of type diglycidyl ether bisphenol A (DGEBA) with 1.15 g/cm^3 density and the hardener (FD 139), composed of triethylenetetramine (TETA) were both supplied by Epoxyfiber.

The size reduction of wastes was achieved by the fine sieving method according to ABNT NBR 7181 [20], in order to obtain three granulometric ranges: coarse (2.000–0.420 mm), medium (0.420–0.075 mm), and fine particles (<0.075 mm). The glass bottles were crushed in a ball mill in order to obtain coarse and medium granulations, and the quartz dust was already fitting the fine granulometry.

2.2. Parameters of Plates Development

To determine the closest-packed mixture, a ternary diagram based on the experimental numeric-modeling grid simplex (simplex-lattice design) (Figure 1), based on the ABNT/MB-3388 Brazilian standard [21], was proposed. Ten (10) different mixtures of the three granulometric ranges were proposed. The proportions are indicated in Figure 1. Each mixture was placed in a 1013.24 cm^3 steel vessel coupled to a 10 kg weight, under 60 Hz of vibration for 10 min.

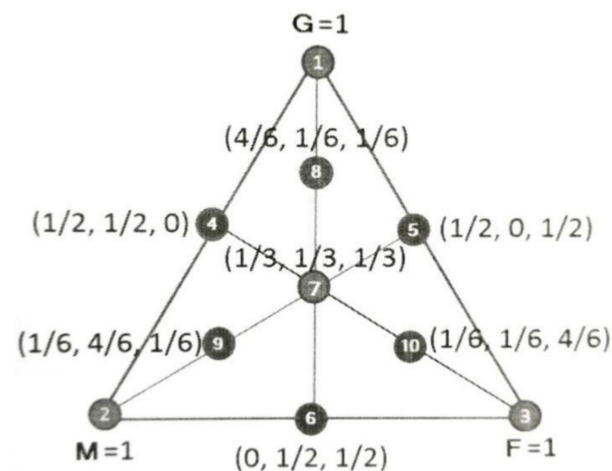


Figure 1. Ternary diagram with the simplex complete cubic model 10 mixtures composition. Proportions of coarse (G), medium (M), and fine (F) particles [7].

The mixture with the greatest vibrated density through packaging was calculated, representing the closest packing of particles, and was chosen for the development of the ENS plates.

The minimum amount of resin (MAR) needed to produce the ENS plates was calculated through the volume void (VV), which is found by Equation (1) [22]:

$$VV\% = \left(1 - \frac{\text{particles apparent dry density}}{\text{glass density} + \text{quartz density}} \right) \times 100 \quad (1)$$

The minimum amount of resin (MAR), represented by the amount of resin enough to fill these volume void, were then calculated through Equation (2) [22]:

$$\text{MAR}\% = \frac{\text{VV}\% \times \rho_{\text{resin}}}{\text{VV}\% \times \rho_{\text{resin}} + (100 - \text{VV}\%) \times \rho_{(\text{glass+quartz})}} \quad (2)$$

2.3. Engineered Stone Plate Development

The ENS plates, with $100 \times 100 \times 10$ mm size dimensions, were produced by the vacuum, vibration, and compression method. The raw materials were dried in an oven for 24 h at 100°C , weighed in the appropriate proportions, and mixed with both the epoxy resin and hardener. The mixture was placed in a mold connected to a vacuum system (600 mmHg), which was on a vibrating table for 2 min. The mold, still under vacuum, was positioned in a hydraulic press, where it was compressed for 20 min under 90°C heating. The ENS plates were cooled to room temperature and removed from the mold. The plates were sanded and then cut with a diamond disc in dimensions required by the standards to perform the physical, chemical, and mechanical tests. The epoxy contents in the ENS were 15%wt (ENS-15) and 20%wt (ENS-20).

2.4. Characterization of Engineered Stone Plates

To perform the physical indices test, 18 specimens of $30 \times 30 \times 30$ mm were cut from the ENS plates. The apparent density, water absorption, and apparent porosity were determined in accordance with Annex B of the ABNT/NBR 155845-2 [23], responsible for classifying stone materials for applications such as coatings in civil construction.

The dilatometry test aims to identify dimensional variations of the specimen under heating conditions. The test was performed on the Netzsch DIL402PC equipment under a heating rate of $10^\circ\text{C}/\text{min}$ and a temperature range of $30\text{--}1000^\circ\text{C}$.

The 3-point bend test was performed according to the Annex F of ABNT/NBR 155845-6 [24] Brazilian standard and UNE-EN 14617-2 Spanish standard [25]. Six (6) specimens of $10 \times 25 \times 100$ mm were tested on the Instron branded universal mechanical testing machine, model 5582, under a 0.25 mm/min loading rate, 100 KN load cell, and 80 mm two-point distance, to evaluate the maximum bending stress, as well as the standard deviation.

Abrasive wear tests were performed according to the ABNT/NBR 12042 Brazilian standard [26], using 2 samples of $70 \times 70 \times 30$ mm, which had their thicknesses measured before and after abrasive wearing suffered in 500 and 1000 m track in a MAQTEST Amsler equipment.

The chemical attack resistance was determined according to an adaptation of Annex H of the standard ABNT/NBR ISO 10545-13 [27]. The attack was performed on 16 specimens with dimensions of $50 \times 50 \times 10$ mm, representing 4 specimens for each one of the 4 attack agents. The specimens were under chemical attack by ammonium chloride and citric acid for 24 h and by hydrochloric acid and potassium hydroxide for 96 h.

The stain resistance was performed on ENS-15 according to an adaptation of the guidelines described in Annex G of ABNT/NBR ISO 10545-14 [28], in addition to the staining agents already listed in the standard, namely penetrating agents (Cr_2O_3 green and Fe_2O_3 red), the oxidizing agent (iodine), and the film-forming agent (olive oil). Common household products were also used: grape juice, ketchup, mustard, and coffee. For each staining agent, 5 polished ENS specimens of approximately $40 \times 20 \times 10$ mm had half of their face covered with the staining agents for 24 h, and the material was then classified according to ease of stain removal.

The salt crystallization test was performed on ENS-15 according to an adaptation of the guidelines described in ABNT/NBR 8.094 [29]. Five 50×50 mm specimens were prepared, washed, and dried in an oven at 70°C for 24 h. The specimens were identified, weighed, measured, and subsequently submerged in a sodium chloride solution for 6 h and oven-dried for 18 h, totaling a 24 h cycle. The process was repeated until 50 cycles were completed.

In the 10th, 30th, and 50th cycles, the samples were analyzed using the Olympus LEXT OLS400 confocal microscope to observe possible surface changes due to exposure to the sodium chloride solution.

The ENS pore characteristics before and after the salt crystallization test were obtained in an automatic mercury injection porosimeter, model Autopore IV 9500, from Micromeritics Instrument Company of America, in $6 \times 6 \times 6$ mm samples. Mercury intrusion and extrusion were investigated under pressures between 0 and 33,000 Psi, which equates to approximately 228 MPa, with pore diameters reading between 0.005 μm and 360 μm .

The ENS fractured surface regions subjected to bending tests were observed through SHIMADZU's Super Scan SSX-550 scanning electron microscope (SEM) for microstructural analysis, at 20 kV of secondary electrons. The samples were prepared using an adhesive carbon tape enveloped by a gold surf. The microstructural analysis is important to determine the quality of the adhesion between the particles and the epoxy resin, as well as the presence of voids.

3. Results and Discussion

3.1. Development Parameters

The vibration densities of the 10 mixtures proposed in Figure 1 are displayed in Table 1.

Table 1. Compositions and vacuum and vibration density of the 10 mixtures proposed for ENS development.

Mixture	Density (g/cm^3)
1	1.253 ± 0.03
2	1.250 ± 0.02
3	1.232 ± 0.03
4	1.510 ± 0.01
5	1.418 ± 0.02
6	1.563 ± 0.01
7	1.676 ± 0.03
8	1.586 ± 0.03
9	1.439 ± 0.02
10	1.625 ± 0.04

As shown in Table 1, the mixture that presented the greatest vibration density was Mixture 7 (1/3 coarse, 1/3 medium, and 1/3 fine particles), representing the closest-packed mixture. Therefore, Mixture 7 was chosen as a proportion of particle sizes for the ENS development.

The MAR was calculated through Equation (2) as 15%wt for the epoxy resin. This amount of resin is considered to be the minimum amount of matrix necessary to fill both interstitial and surface voids of the closest-packed mixture.

The ENS plates were produced with 1/3 of coarse particles of glass waste, 1/3 of medium particles of glass waste, and 1/3 of fine particles of quartz waste. Plates were produced with an amount of 15%wt epoxy resin (ENS-15), corresponding to the MAR, and also with 20%wt (ENS-20) of epoxy resin, aiming to verify whether the addition of resin would result in a more effective void filling that would be determined by its mechanical properties.

3.2. Physical Indices

Table 2 presents the physical indices (apparent density, water absorption, and apparent porosity) results found after testing 18 specimens of both ENS-15 and ENS-20.

Table 2. Physical properties of apparent density, water absorption, and apparent porosity of ENS-15 and ENS-20.

Engineered Stone	Density (g/cm ³)	Water Absorption (%)	Apparent Porosity (%)
ENS-15	2.26 ± 0.01	0.10 ± 0.01	0.21 ± 0.03
ENS-20	2.14 ± 0.01	0.12 ± 0.01	0.25 ± 0.03

As can be seen in Table 2, by modifying the amount of resin, a difference in the physical indices was observed. ENS-20 had density values lower than ENS-15, which is due to the fact that the resin content increased, hence a decrease in the amount of waste. The rise in water absorption and porosity values observed in ENS-20 is explained by the resin binding action that brings the particles together. More resin means fewer waste particles in the mixture, forming more empty spaces, called voids, increasing both apparent porosity and water absorption.

Lee et al. [14] developed engineered stone based on glass and granite wastes under different conditions of pressure, temperature, and vacuum. In their work, the results ranged between 2.03 and 2.45 g/cm³ for density and from 0.01 to 0.20% for water absorption. By observing Table 2, one can notice that the density and water absorption values found for both ENS-15 and ENS-20RAVQ 20% are within the range found by Lee et al.

A commercial stone named Stellar™, also produced by EcologicStone, the same company that supplied the quartz dust for this work, was characterized in the work of Carvalho et al. [15], presenting 2.38 g/m³ density, 0.18% water absorption, and 0.44% apparent porosity. Both ENS-15 and ENS-20 are relatively lower than the commercial stone, with similar porosity and water absorption, indicating that the produced rock can be an alternative to replace the commercial Stellar™ stone, not only reusing the wastes but also with structure and logistic savings because of the lower density.

According to Chiodi and Rodrigues [30], lining or facing civil construction materials classified as high quality must have porosity below 0.5%. As can be seen in Table 2, the porosity values found for both ENS-15 and ENS-20 are below this value, evidencing the high quality of both engineered stones produced for coating applications.

As ENS-15 showed better physical indices, it was chosen to be tested for its mechanical and thermal properties.

3.3. Dilatometry Test

Numerous materials present dimensional variations after being exposed to a heating period, presenting dimensional variations under the effect of the contraction and expansion phenomena in their structures. These variations take place due to physical and chemical events that occur in the structures and chemical composition of their materials. In the development of engineered stone, thermal transformations occur in the curing stage because of the matrix/waste polymerization reaction [31].

The ENS, composed of glass and quartz in the epoxy matrix, had excellent test stability and resistance, probably due to the aggregate's properties and characteristics at high temperatures. Figure 2 presents the ENS-15 dilatometry analysis.

In Figure 2, one can observe the structural behavior of ENS-15 in a heated environment in a range of temperature from 0° to 1000 °C, identifying the structural phenomena presented such as the body temperature at the exact moment.

In the range of 0–300 °C, it is possible to see the adaptation of materials to the heated environment, favoring pore expansion and the structure's moisture loss, in addition to a molecular chemical activation, which causes movement expanding the entire structure. Owing to the adaptation, at 338 °C, the structure contracts, which is followed by an expansion at 362.6 °C and a significant decline at 382.4 °C, a temperature where the resin begins to decompose, with a weight loss demonstrated in previous works [17].

According to Silva et al. [17], the epoxy resin thermogravimetry curve registers the first 70% weight loss at about 380 °C due to the resin's decomposition. Subsequently, at 382.4 °C,

there is a weight loss that continues until the end of the process, at 550 °C [17]. After 600 °C, the structure undergoes another contraction, and there is a total weight loss because of the resin and the melting temperature of the waste glass, which is around 600–1117 °C, and of the quartz dust, which, at around 870 °C, becomes tridymite, a high-temperature silica polymorph [17,31].

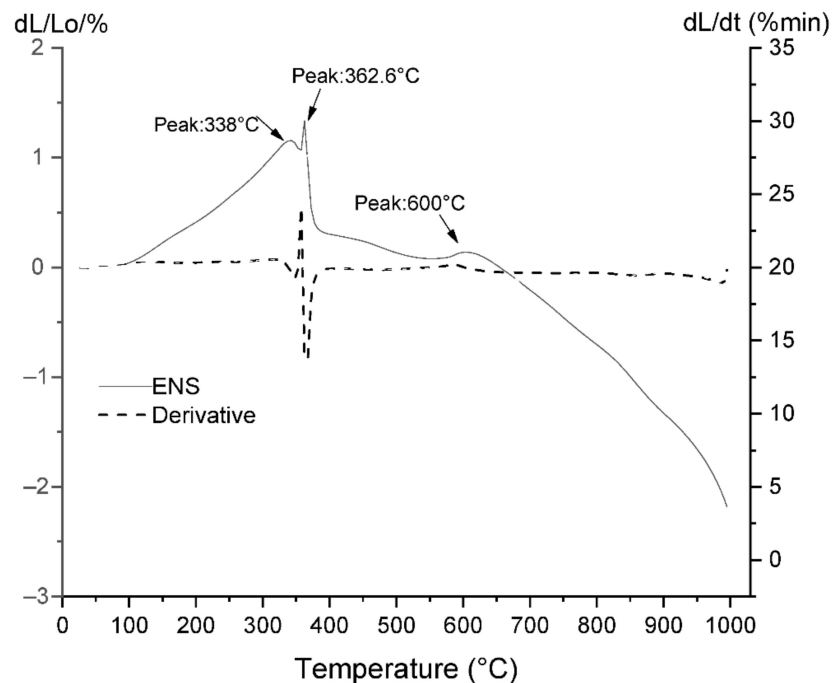


Figure 2. Dilatometry curve of ENS-15.

3.4. Three-Point Bend Strength

Table 3 presents the three-point bend strength values of ENS-15 and pure epoxy resin.

Table 3. Three-point bend strength of ENS-15 and epoxy resin.

Materials	3-Point Bend Strength (MPa)
ENS-15	33.54 ± 4.05
Epoxy	93.6 ± 4.70

Figure 3 shows the stress vs. strain curves obtained by the three-point bending test of ENS-15 developed and of the pure epoxy resin. Mechanical strength, or the stress at which the material breaks, is the most important property for structural materials.

The mechanical bending resistance of ENS-15 was 33.5 ± 4.0 MPa, with a strain ranging from 0.0 to 0.3.

When comparing the ENS bending strength results of those found by Carvalho et al. [15] for Stellar™ (36.61 ± 2.48 MPa) with those also found by Carvalho et al. [6], artificial stone developed with quarry waste and 15% epoxy resin (32 ± 2 MPa), and by Gomes et al. [16], AOS artificial stone developed with brick waste and quarry dust with 20% epoxy resin (30 ± 3 MPa), it is noticeable that the values for ENS-15 are in accordance with those found by other authors for similar materials.

According to Chiodi Filho and Rodriguez [30], ornamental stones used as coatings in civil construction, with bending strength above 20 MPa, are classified as highly resistant materials. As ENS-15 presented flexural strength above this value, it can be classified as a high-strength engineered stone, enabling it to be used on tops and countertops without restriction, as well as in internal and external walls.

The GSO ASTM C503/2015 [32] standard specifies that calcitic marble bend strength must be greater than 7 MPa. The bend strength values found by the ENS developed in this work represent about five times this value. Therefore, it is possible to affirm that the material developed represents a formidable alternative to replace calcitic marble, which could result in material savings, since the greater resistance would make it possible to produce the same materials with smaller dimensions.

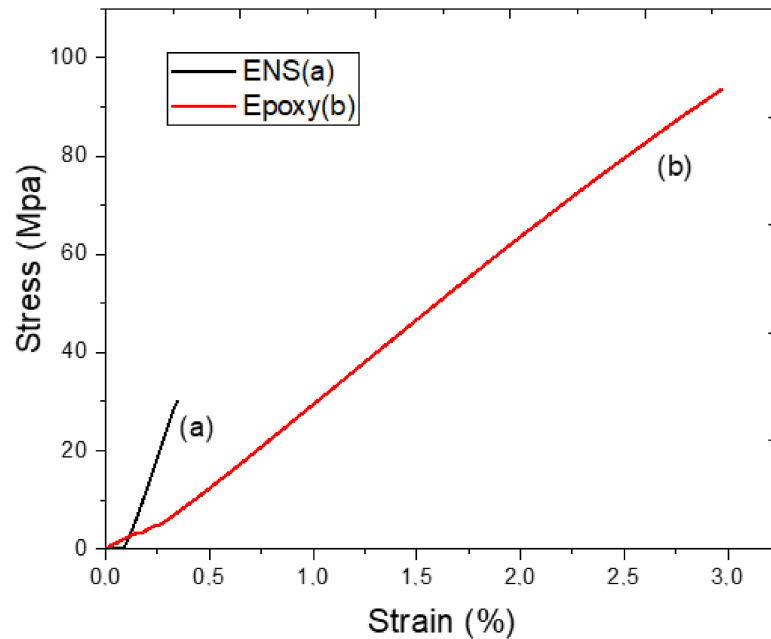


Figure 3. Mechanical behavior of ENS-15 and the pure epoxy resin in 3-point bend strength tests.

3.5. Abrasive Wear Test

Table 4 presents the thickness reduction of ENS-15 after two specimens were subjected to abrasive wear tests at two running distances, 500 and 1000 m.

Table 4. Amsler abrasive wear through with thickness reduction of ENS-15.

Material	Thickness Reduction (mm)	
	500 m	1000 m
ENS-15	1.41 ± 0.22	2.86 ± 0.25

For artificial stones to be applied for civil construction, there are no requirements, standards, or limits to thickness reduction in abrasive wear tests. Chiodi Filho and Rodrigues [30] proposed technological parameters for the use of artificial stones in pavements. The authors recommended that pavements with low traffic should display wear thickness reduction lower than 6 mm, medium traffic should be lower than 3 mm, and heavy traffic lower than 1.5 mm. Based on the described parameters, the novel ENS-15 (Table 4) can be used for medium traffic pavement, since it presented a thickness reduction below 3 mm on the 1000 m track.

3.6. Chemical Attack Resistance

Table 5 presents the relative weight loss (%) suffered by the specimens ENS-15 and ENS-20 after 24 h or 96 h under chemical attack. The reagents simulate the composition of some substances, such as cleaning products and food or atmospheric acids, that would possibly be in contact with the engineered stone if applied as a coating.

Table 5. Relative weight loss after 24 h/96 h of chemical attack of ENS-15 specimens.

Reagents	Relative Weight Loss (%)	Time Span
NH ₄ Cl	0.07 ± 0.01	24 h
C ₆ H ₈ O ₇ (citric acid)	0.18 ± 0.04	24 h
HCl	0.41 ± 0.02	96 h
KOH	0.08 ± 0.01	96 h

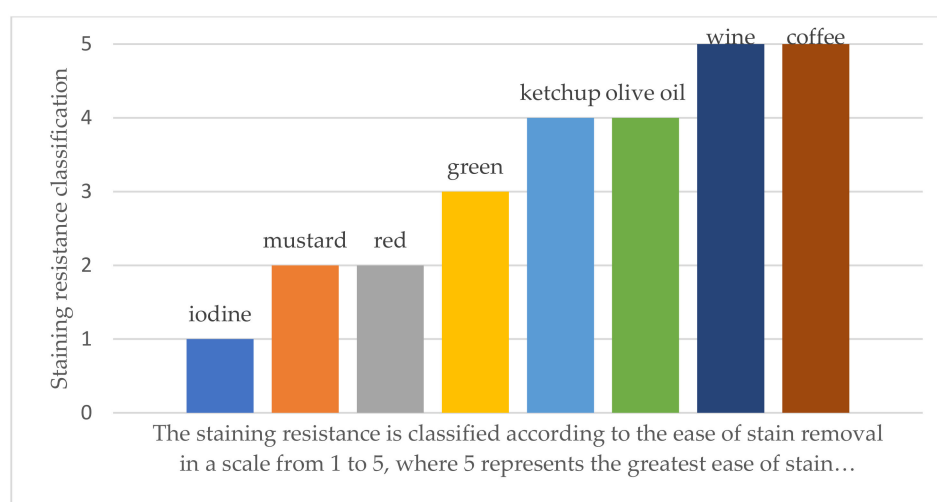
After observing the results presented in Table 5, it can be seen that the ENS produced had a smaller weight loss when attacked by basic reagents than when attacked by acidic ones, probably due to the matrix, since epoxy resin has a high resistance to chemical agents, especially alkali [33].

ENS-15 had a small relative weight loss in the face of chemical attacks, which can be attributed to the fact that the glass, quartz, and epoxy resin are materials that present certain chemical stability. Possibly, the glass, as its original application was beverage packaging, had a more chemically inert composition. Quartz at room temperature presents a stable phase of silica and is also, by nature, a chemically stable material [30].

Gomes et al. [16] evaluated the behavior of their AOS artificial stone also agglomerated by epoxy resin under chemical attack with the same agents used in the present work. However, the authors evaluated chemical attack resistance for all reagents for only 24 h, while in this present work, some chemical attack reagents acted for 96 h according to the standard [32]. Still, the reagent that caused the greatest weight loss was HCl, corroborating the conclusions of Gomes et al. [16].

3.7. Stain Resistance

Figure 4 presents a graph illustrating the stain resistance behavior of ENS-15 according to a scale of the difficulty degree in removing the stains after the cleaning procedures described in the standard [28]. In this scale, Number 5 represents the easiest stain removal, and Number 1 represents the harder stain removal. In fact, a stain at Number 1 is one that remains even after all the cleaning procedures.

**Figure 4.** Stain resistance behavior of ENS-15 after 24 h covered with the staining agents.

ENS-15 showed high stain resistance for agents such as wine and coffee, which were cleaned only with hot water. Olive oil and ketchup stains were easily removed by detergent, and, after cleaning with an abrasive paste, the green agent (Cr₂O₃) stain was also removed. For cleaning the other stains left by red (Fe₂O₃), mustard, and iodine, the specimens were submerged in acidic solution for 24 h. ENS-15 did not show iodine stain resistance because this stain remained at Number 1, as shown in Figure 4.

Peixoto et al. [15,22] also developed an artificial stone with the incorporation of glass waste, but with another type of glass from the industrial lamination stage. They evaluated its stain resistance with the same method and same staining agents, but no stain remained after the test.

Borsellino et al. [34] also evaluated the stain resistance of their artificial marbles developed with marble and epoxy resin and also with polyester resin. However, they used different staining agents and another method. It was pointed out by the authors that plates with more epoxy resin content suffered fewer surface alterations after the stain resistance test, which was attributed to the higher epoxy resin stain resistance.

Stain resistance is kindred to surface pores because, after polishing the stone surface, the internal pores become surface pores, also known as open pores, which hinder the removal of stains [22].

The stain resistance test is important to evaluate the quality of engineered stones because of its application, which takes aesthetics into account, and because of its use in kitchens, bathrooms, and laboratory countertops, which constantly expose ENS to staining substances.

3.8. Salt Crystallization Test

Table 6 shows the ENS weight before the test and its weight after the salt crystallization cycles. In each cycle, the samples were submerged in saline water and taken to an oven for drying, respecting their respective times. It can be observed that there was a small weight variation during the cycles, which indicates little absorption of salinized water, evidencing the low porosity shown in the physical index.

Table 6. Weight variation after 10, 30, and 50 cycles of ENS salt crystallization test.

Test Conditions	Weight Variation (g)	Weight Variation (%)
10 cycles	0.02 ± 0.01	$+0.04 \pm 0.02$
30 cycles	0.06 ± 0.03	$+0.09 \pm 0.05$
50 cycles	0.50 ± 0.30	$+0.87 \pm 0.54$

Figure 5 shows the engineered stone's pore distribution before and after the salt crystallization test.

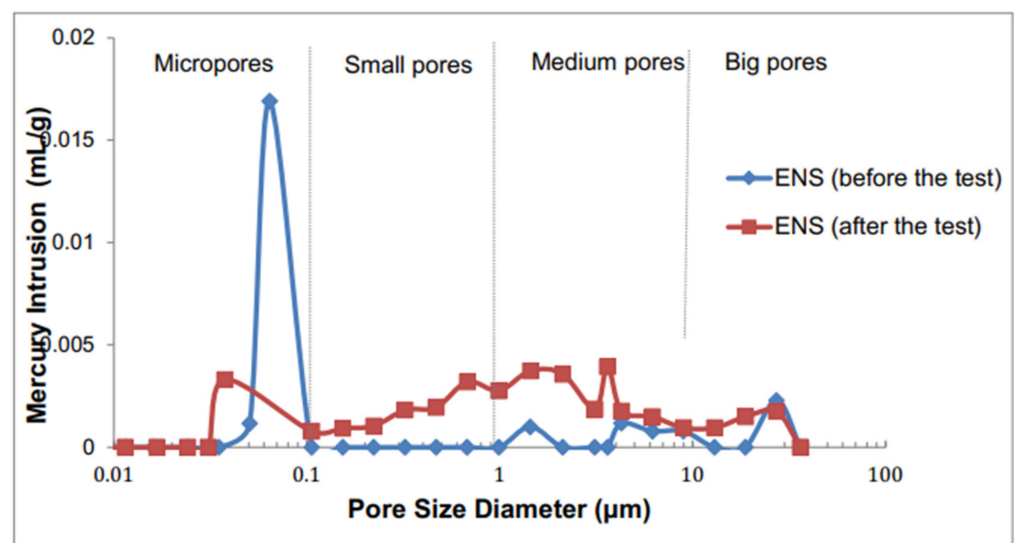


Figure 5. Pore diameter distribution of ENS before and after the salt crystallization test.

The ENS had four pore diameter ranges after the test, large, medium, small, and micropores, whereas the intact ENS had no range of small pores. Mercury intrusion and

volume increased for ENS in the micropore range, probably due to sample failures. The intact ENS obtained a 0.005 mL/g mercury intrusion volume and 0.89% porosity, and the ENS after the test had 0.0064 mL/g mercury intrusion and 1.29% porosity, indicating the appearance of new pores.

The diameter of pores and the mercury intrusion volume increased in all diameter ranges. The elevation in mercury intrusion and pore diameter can be attributed to temperature variations and the crystallization of salts in the pores that expand, producing tensions that enlarge their diameter.

The studies by Benavente et al. [35] and Yu and Oguchi [36] reported that saline solutions could come from external sources, such as natural salts or anthropogenic discharges, such as marine spray, pesticides, and wastes from fossil fuel combustion. The exposure of artificial stones to these external saline solutions could induce a capillarity and porosity increase, consequently impairing the material's mechanical properties.

The literature also reports an enormous discrepancy between the limited damage observed in the laboratory and the severe deterioration that happens when artificial stones are contaminated with NaCl from external sources. When considering the pore damage due to salt crystallization, the lower destructive potential of NaCl in the laboratory could be attributed to its tendency to supersaturate [37], which can be observed in Table 6, as, despite repetitive cycles, there was no considerable weight variation in the tested specimens.

Flat and three-dimensional micrographs of the ENS before and after the test were obtained with confocal microscopy during cycles of 10, 30, and 50, as shown in Figures 6 and 7.

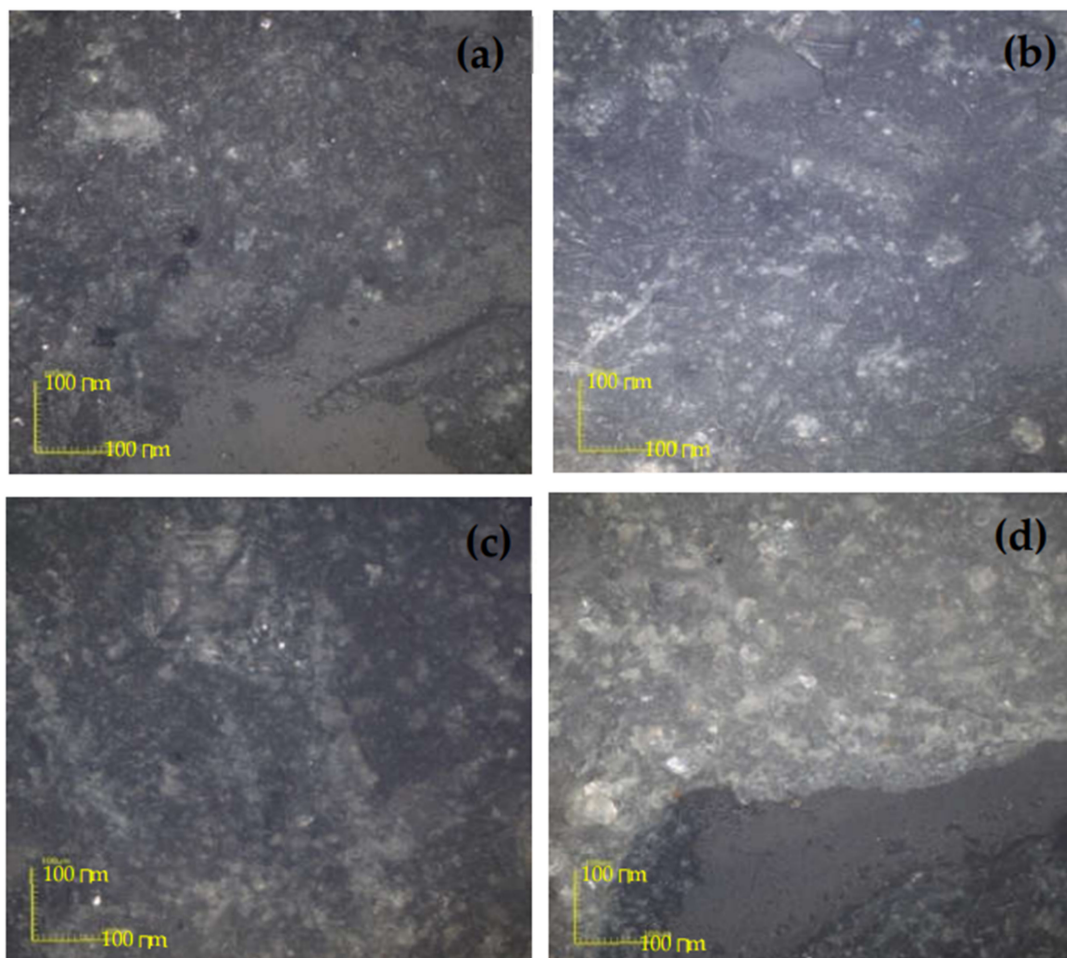


Figure 6. Photomicrograph of ENS under the salt crystallization test: ENS before test (a), after 10 cycles (b), after 30 cycles (c), and after 50 cycles (d), with 430× magnification.

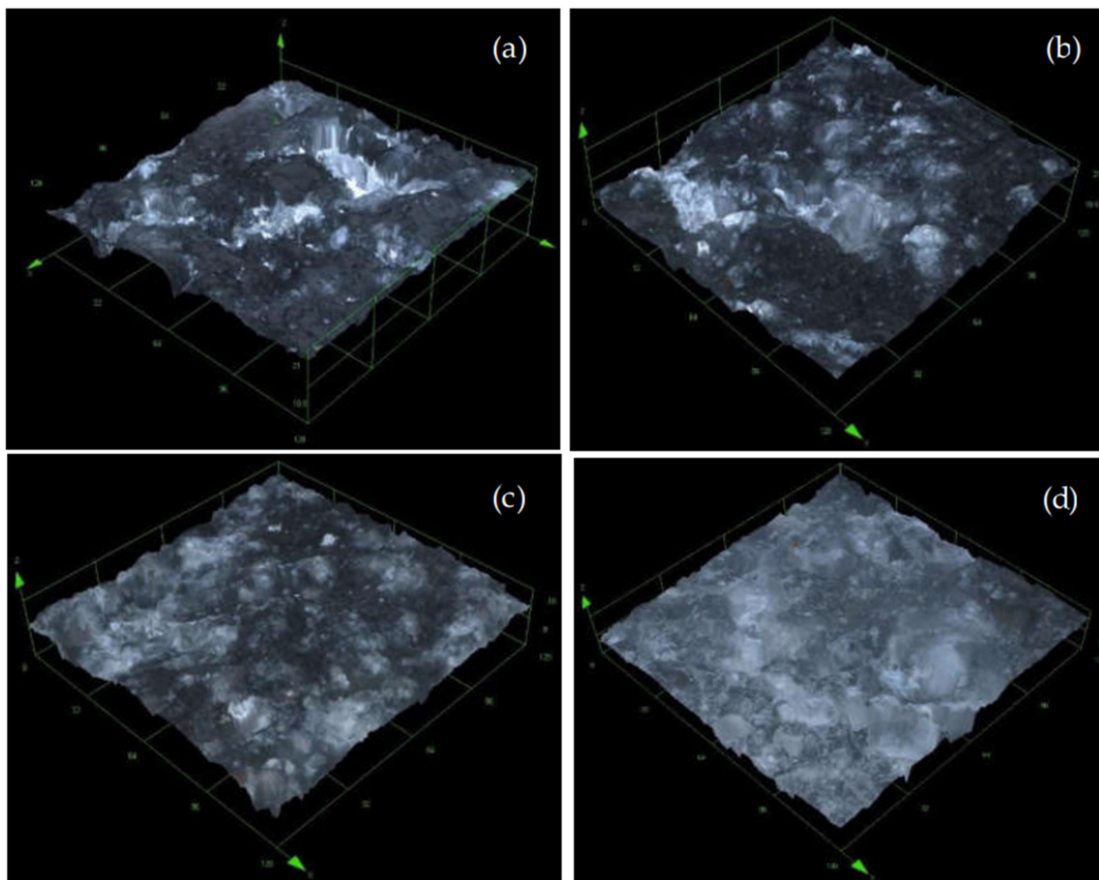


Figure 7. Three-dimensional photomicrograph of ENS under the salt crystallization test: ENS before test (a), after 10 cycles (b), after 30 cycles (c), and after 50 cycles (d), with $430\times$ magnification.

As displayed in Figure 6, ENS after 50 cycles (Figure 6d) underwent a greater change on the surface, evidenced by the more whitish and yellowish color. The accelerated degradation in the laboratory brings the brightness loss, yellowing, porosity, microcracks, and the mineral alteration state caused by the joint action of factors such as temperature and sodium presence (saline water). This leads to salt crystallization in the exposed pores, generating tensions responsible for increasing the diameter of pores and physical origin surface changes [38]. At 10 and 30 cycles, there was no significant surface change.

The three-dimensional photomicrographs (Figure 7) show that the ENS after 30 cycles (Figure 7c) had a greater pore or cavity number, being more pronounced in the ENS after 50 cycles (Figure 7d), indicating the loss of surface cohesion as the number of cycles rise, leading to the detachment of the material in the form of dust and/or small particles [38].

3.9. SEM Observations

Figure 8a,b displays the ENS micrographs of surface fracture obtained by SEM.

In Figure 8, it is possible to notice that the presence of pores or cavities in the material (white arrows) is quite reduced, which was already expected due to the low porosity and water absorption and to the manufacturing process that uses vibration, compaction, and vacuum.

The occurrence of displaced particles (Figure 8a) of the matrix can also be observed, as indicated by the arrow. The voids in the interface region point to this displacement. There was little displacement of waste grains (Figure 8a,b), confirming the efficient wetting [17].

The compaction enhances the settlement and adhesion of particles, and the vacuum assists the resin to better penetrate the interstices of the waste particles, filling the void volume [3], which is clearly seen in the micrograph, by a good interfacial adhesion between the waste particles and the resin. The good interfacial interaction is evidence of effective

interfacial wetting of the resin, which is directly related to the improvement of the material's mechanical properties, as reported by Miller et al. [39] and Debnath et al. [40]. Figure 8a,b both show intergranular fracture surfaces with evidence of mechanical stress failure, since the fracture cracks pass through the grains indicated by the arrow.

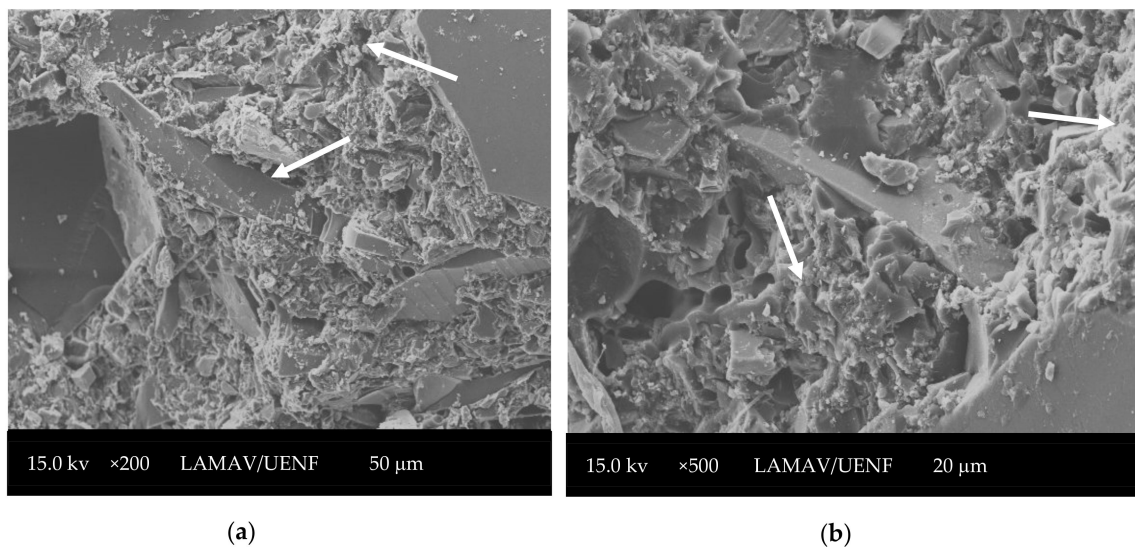


Figure 8. ENS-15 scanning electron fractured surface micrographs with different magnifications: (a) 200× and (b) 500×.

4. Conclusions

This work aimed to develop an ENS based on glass packaging waste, quartz dust, and epoxy resin (ENS-15 and ENS-20) through vacuum vibration and compression, as well as to determine its physical and mechanical properties.

From the experimental results obtained in this study, the following conclusions can be drawn:

- ENS-15 and ENS-20 are materials of low density, with 2.26 and 2.24 g/cm³, respectively. The water absorption was 0.10 and 0.12%, considering both as low absorption ENS materials;
- Both ENS-15 and 20 are high-quality coating materials for lining civil construction due to their porosity below 0.5%;
- ENS-15 is a highly resistant material, owing to its 33.5 MPa bend strength, which exceeds the recommended value of at least 20 MPa for construction coating materials;
- ENS with a 2.86 mm thickness reduction on the 1000 m track can be used for pavement on floors with medium traffic, since it presented thickness reduction below the recommended value for this type of material;
- The ENS displayed good chemical stability, proved by its low relative weight loss after the chemical attack test.
- The ENS is likely to be used as a coating in kitchens and bathrooms, since it is highly resistant to some staining agents except iodine;
- SEM micrographs showed the low presence of pores and an optimal waste/resin interfacial adhesion, corroborating the physical indices and bend strength results.
- Therefore, the development of ENS based on glass, quartz dust, and epoxy resin has the potential to be used as an alternative material, competing with both natural and commercial artificial stones, which are currently marketed in civil construction, leading to environmental and economical improvements.

Author Contributions: Conceptualization, C.M.F.V. and E.A.S.C.; methodology, G.N.S.B., C.M.F.V., and E.A.S.C.; Validation, G.N.S.B., V.d.S.d.S., M.L.P.M.G., and E.A.S.C.; investigation, G.N.S.B. and V.d.S.d.S.; data curation, G.N.S.B.; writing—original draft preparation, G.N.S.B.; writing—review and editing, G.N.S.B., V.d.S.d.S., and E.A.S.C.; supervision, E.A.S.C. and A.R.G.d.A.; project administration, S.N.M. and C.M.F.V. funding acquisition, S.N.M., A.R.G.d.A., and C.M.F.V. All authors have read and agreed to the published version of the manuscript.

Funding: This research was funded by FAPERJ (Grant Number: E-26/200.847/2021) and CNPQ (Grant Number: 301634/2018-1). The participation of A.R.G.A. was sponsored by FAPERJ through the research fellowships Proc. Nos.: E-26/210.150/2019, E-26/211.194/2021, E-26/211.293/2021, and an-dE-26/201.310/2021, and by CNPq through the research fellowship PQ2 307592/2021-9.

Institutional Review Board Statement: Not applicable.

Informed Consent Statement: Not applicable.

Data Availability Statement: Not applicable.

Conflicts of Interest: The authors declare no conflict of interest.

References

- Harrison, E.; Berenjian, A.; Seifan, M. Recycling of waste glass as aggregate in cement-based materials. *Environ. Sci. Ecotechnol.* **2020**, *4*, 100064. [[CrossRef](#)]
- Bisht, K.; Syed Ahmed Kabeer, K.I.; Ramana, P.V. Gainful utilization of waste glass for production of sulphuric acid resistance concrete. *Constr. Build. Mater.* **2020**, *235*, 117486. [[CrossRef](#)]
- Dong, W.; Li, W.; Tao, Z. A comprehensive review on performance of cementitious and geopolymeric concretes with recycled waste glass as powder, sand or cullet. *Resour. Conserv. Recycl.* **2021**, *172*, 105664. [[CrossRef](#)]
- Guo, P.; Meng, W.; Nassif, H.; Gou, H.; Bao, Y. New Perspectives on Recycling Waste Glass in Manufacturing Concrete for Sustainable Civil Infrastructure. *Constr. Build. Mater.* **2020**, *257*, 119579. [[CrossRef](#)]
- Sadowski, L.; Piechówka-Mielnik, M.; Widziszowski, T.; Gardynik, A.; Mackiewicz, S. Hybrid ultrasonic-neural prediction of the compressive strength of environmentally friendly concrete screeds with high volume of waste quartz mineral dust. *J. Clean. Prod.* **2019**, *212*, 727–740. [[CrossRef](#)]
- Santos Carvalho, E.A.; de Figueiredo Vilela, N.; Monteiro, S.N.; Fontes Vieira, C.M.; da Silva, L.C. Novel Artificial Ornamental Stone Developed with Quarry Waste in Epoxy Composite. *Mater. Res.* **2018**, *21* (Suppl. S1), e20171104. [[CrossRef](#)]
- Barreto, G.N.S.; Babisk, M.P.; Delaqua, G.C.G.; Gadioli, M.C.B.; Vieira, C.M.F. Evaluation on the Effect of the Incorporation of Blends of Fuel and Fluxing Wastes. *Mater. Res.* **2019**, *22* (Suppl. S1), e20190199. [[CrossRef](#)]
- Adedirán, A.; Lemougna, P.N.; Yliniemi, J.; Tanskanen, P.; Kinnunen, P.; Roning, J.; Illikainen, M. Recycling glass wool as a fluxing agent in the production of clay- and waste-based ceramics. *J. Clean. Prod.* **2021**, *289*, 125673. [[CrossRef](#)]
- Gao, X.; Yu, Q.; Li, X.S.; Yuan, Y. Assessing the modification efficiency of waste glass powder in hydraulic construction materials. *Constr. Build. Mater.* **2020**, *263*, 120111. [[CrossRef](#)]
- Cordon, H.C.F.; Cagnoni, F.C.; Ferreira, F.F. Comparison of physical and mechanical properties of civil construction plaster and recycled waste gypsum from São Paulo, Brazil. *J. Build. Eng.* **2019**, *22*, 504–512. [[CrossRef](#)]
- Kumar, S.; Gupta, R.C.; Shrivastava, S. Long term studies on the utilization of quartz sandstone wastes in cement concrete. *J. Clean. Prod.* **2017**, *143*, 634–642. [[CrossRef](#)]
- Lameiras, F.S.; da Silva, G.D.L. Methodology to control the influence of processing factors during composite stone fabrication. *Rem Rev. Esc. Minas* **2015**, *68*, 69–75. [[CrossRef](#)]
- Lee, D.J.; Shin, I.J. Effects of vacuum, mold temperature and cooling rate on mechanical properties of press consolidated glass fiber/PET composite. *Compos. Part A Appl. Sci. Manuf.* **2002**, *33*, 1107–1114. [[CrossRef](#)]
- Lee, M.-Y.; Ko, C.-H.; Chang, F.-C.; Lo, S.-L.; Lin, J.-D.; Shan, M.-Y.; Lee, J.-C. Artificial stone slab production using waste glass, stone fragments and vacuum vibratory compaction. *Cem. Concr. Compos.* **2008**, *30*, 583–587. [[CrossRef](#)]
- Carvalho, E.A.S.; Marques, V.R.; Rodrigues, R.J.S.; Ribeiro, C.E.G.; Monteiro, S.N.; Vieira, C.M.F. Development of Epoxy Matrix Artificial Stone Incorporated with Sintering Residue from Steelmaking Industry. *Mater. Res.* **2015**, *18* (Suppl. S2), 235–239. [[CrossRef](#)]
- Gomes, M.L.P.M.; Carvalho, E.A.S.; Sobrinho, L.N.; Monteiro, S.N.; Rodriguez, R.J.S.; Vieira, C.M.F. Production and characterization of a novel artificial stone using brick residue and quarry dust in epoxy matrix. *J. Mater. Res. Technol.* **2018**, *7*, 492–498. [[CrossRef](#)]
- Silva, F.S.; Ribeiro, C.E.G.; Rodriguez, R.J.S. Physical and Mechanical Characterization of Artificial Stone with Marble Calcite Waste and Epoxy Resin. *Mater. Res.* **2017**, *21*, e20160377. [[CrossRef](#)]
- Da Cunha Demartini, T.J.; Rodríguez, R.J.S.; Silva, F.S. Physical and mechanical evaluation of artificial marble produced with dolomitic marble residue processed by diamond-plated bladed gang-saws. *J. Mater. Res. Technol.* **2018**, *7*, 308–313. [[CrossRef](#)]

19. Gomes, M.L.P.; Carvalho, E.A.; Demartini, T.J.; de Carvalho, E.A.; Colorado, H.A.; Vieira, C.M.F. Mechanical and physical investigation of an artificial stone produced with granite residue and epoxy resin. *J. Compos. Mater.* **2021**, *55*, 1247–1254. [[CrossRef](#)]
20. Brazilian Association of Technical Norms—ABNT. Soil—Grain Size Analysis ABNT NBR 7181. September 2016. Available online: <https://www.abntcatalogo.com.br/> (accessed on 20 March 2022).
21. Brazilian Association of Technical Norms—ABNT. NBR MB 3388: Soil—Determination of Minimum Index Void Ratio of Cohesionless Soils—Method of Test. Rio de Janeiro. 1991. Available online: <https://www.abntcatalogo.com.br/> (accessed on 20 March 2022).
22. Peixoto, J.; Santos Carvalho, E.A.; Menezes Gomes, M.L.P.; da Silva Guimarães, R.; Monteiro, S.N.; de Azevedo, A.R.G.; Fontes Vieira, C.M. Incorporation of Industrial Glass Waste into Polymeric Resin to Develop Artificial Stones for Civil Construction. *Arab. J. Sci. Eng.* **2022**, *47*, 4313–4322. [[CrossRef](#)]
23. Brazilian Association of Technical Norms—ABNT. ABNT NBR15845-2: Rocks for Cladding. Part 2: Determination of Bulk Density, Apparent Porosity and Water Absorption. August 2015. Available online: <https://www.abntcatalogo.com.br/> (accessed on 20 March 2022).
24. Brazilian Association of Technical Norms—ABNT. ABNT NBR15845-6: Rocks for Cladding. Part 6: Determination of Modulus of Rupture (Three Point Bending). July 2015. Available online: <https://www.abntcatalogo.com.br/> (accessed on 20 March 2022).
25. Spanish Association of Standards and Certification. *UNE-EN14617-2-08*; Test Methods. Part 2: Determination of the Flexural Strength; Spanish Association of Standards and Certification: Madrid, Spain, 2008.
26. Brazilian Association of Technical Norms—ABNT. ABNT NBR12042: Inorganic Materials—Determination of the Resistance to Abrasion. December 2012. Available online: <https://www.abntcatalogo.com.br/> (accessed on 20 March 2022).
27. Brazilian Association of Technical Norms—ABNT. ABNT NBRISO10545-13: Ceramic Tiles—Part 13: Determination of Chemical Resistance. July 2020. Available online: <https://www.abntcatalogo.com.br/> (accessed on 20 March 2022).
28. Brazilian Association of Technical Norms—ABNT. ABNT NBRISO10545-14: Ceramic Tiles—Part 14: Determination of Resistance to Stains. November 2017. Available online: <https://www.abntcatalogo.com.br/> (accessed on 20 March 2022).
29. Brazilian Association of Technical Norms—ABNT. ABNT NBR 8.094: Coated and Uncoated Metallic Material—Corrosion from Salt Fog Exposure—Test Method. 1983. Available online: <https://www.abntcatalogo.com.br/> (accessed on 20 March 2022).
30. Chiodi Filho, C.; de Paula Rodrigues, E. *Guide Application of Stone Coverings*; ABIROCHAS: São Paulo, Brazil, 2009.
31. Carvalho, E.A.S.; da Silva de Souza, V.; Barreto, G.N.S.; Monteiro, S.N.; Rodriguez, R.J.S.; Vieira, C.M.F. Incorporation of Porcelain Powder and Mineral Wastes in Epoxy Matrix for Artificial Stone Purchase. In *Characterization of Minerals, Metals, and Materials*; Springer: Cham, Switzerland, 2021; pp. 435–443. [[CrossRef](#)]
32. American Society for Testing and Materials—ASTM. *ASTM C503-03*; Standard Specification for Marble Dimension Stone (Exterior); ASTM: West Conshohocken, PA, USA, 2003.
33. Tesser, E.; Lazzarini, L.; Bracci, S. Investigation on the chemical structure and ageing transformations of the cycloaliphatic epoxy resin EP2101 used as stone consolidant. *J. Cult. Herit.* **2018**, *31*, 72–82. [[CrossRef](#)]
34. Borsellino, C.; Calabrese, L.; di Bella, G. Effects of powder concentration and type of resin on the performance of marble composite structures. *Constr. Build. Mater.* **2009**, *23*, 1915–1921. [[CrossRef](#)]
35. Benavente, D.; García del Cura, M.A.; Fort, R.; Ordóñez, S. Durability estimation of porous building stones from pore structure and strength. *Eng. Geol.* **2004**, *74*, 113–127. [[CrossRef](#)]
36. Yu, S.; Oguchi, C.T. Role of pore size distribution in salt uptake, damage, and predicting salt susceptibility of eight types of Japanese building stones. *Eng. Geol.* **2010**, *115*, 226–236. [[CrossRef](#)]
37. Lubelli, B.; Cnudde, V.; Diaz-Goncalves, T.; Franzoni, E.; van Hees, R.P.J.; Ioannou, I.; Menendez, B.; Nunes, C.; Siedel, H.; Stefanidou, M.; et al. Towards a more effective and reliable salt crystallization test for porous building materials: State of the art. *Mater. Struct.* **2018**, *51*, 55. [[CrossRef](#)]
38. Costa, K.O.B. *Microstructural, Physical and Mechanical Characterization and Durability of Fluminense Ornamental Stones*; Campos dos Goytacazes: Lisbon, Portugal, 2021. (In Portuguese)
39. Miller, J.D.; Ishida, H.; Maurer, F.H.J. Dynamic-mechanical properties of interfacially modified glass sphere filled polyethylene. *Rheol. Acta* **1988**, *27*, 397–404. [[CrossRef](#)]
40. Debnath, S.; Ranade, R.; Wunder, S.; McCool, J.; Boberick, K.; Baran, G. Interface effects on mechanical properties of particle-reinforced composites. *Dent. Mater.* **2004**, *20*, 677–686. [[CrossRef](#)]